Identification of Key Rab Proteins in Human Gonadotropin-Releasing Hormone Receptor Anterograde Trafficking

A Senior Thesis submitted to
the Faculty of the Department of Biology,
Colorado College
by

Kayla Warfield

Bachelor of Arts Degree in Biology

May 19, 2014

Approved by:

_____

Primary Thesis Advisor – Dr. Ralph Bertrand

_____

Secondary Thesis Advisor – Dr. Darrell Killian

TABLE OF CONTENTS:

I. ABSTRACT

The mechanism of vesicular trafficking is a process that is not well understood, but it is critical to the operation and function of a cell. Rab proteins guide anterograde (ER to plasma membrane) and retrograde (plasma membrane to ER) directional vesicular movement, but most Rab proteins have been shown to have varying trafficking roles with membrane-bound vesicle movement, tethering, and fusion specific to the cargo within the vesicle. This study aimed to identify Rab proteins that are involved in anterograde trafficking of human gonadotropin-releasing hormone receptor (GnRHR). Plasmids encoding Rab GTPase DNA, along with human GnRHR DNA, were transfected into Cos-7 African green monkey kidney tumor cells *in vitro*. Cells were grown in tritium inositol and upon stimulation of GnRHR, inositol phosphates (IP) containing radioactive markers were synthesized. A radioimmunoassay was conducted to determine total presence of inositol phosphate (IP), a marker that correlates with GnRHR presence at the plasma membrane. Rab6 and Rab3a were identified as significantly increasing IP levels, an indication of higher presence of GnRHR at the cell membrane and anterograde activity. Moving forward, further research will be pursued to find additional Rab GTPase proteins involved in anterograde trafficking and their specific function and localization. Understanding the pathway of GnRHR to the plasma membrane could improve therapeutic treatments for hypogonadotropic hypogonadism, a disease caused by loss-of-function of GnRHR due to a failure of expression at the cell membrane.

II. INTRODUCTION

G Protein-Coupled Receptors

G protein-coupled receptors (GPCRs) are cell surface proteins that regulate physiological responses and are thus the major target of therapeutic drugs today. While there are more than 600 distinct GPCRs, all GPCRs share a molecular structure consisting of seven transmembrane alpha helices forming a hydrophobic core, an extracellular N-terminus and an intracellular C-terminus (Lachance et al., 2011). The intracellular C-terminal tail is very conserved among GPCRs, while the section crossing the membrane is semi-conserved and the extracellular regions vary greatly.

Once ligand binding occurs on the extracellular binding site of the GPCR, a conformational change in the receptor occurs, leading to GPCR coupling to heterotrimeric G proteins, often after dimerization or oligomerization of the GPCRs at the plasma membrane. The G protein is activated by a guanine nucleotide exchange factor replacing GDP with a GTP on the α-subunit. A signal cascade ensues, activating downstream effectors such as adenylyl cyclases, phospholipases, protein kinases, inositol phosphates and ion channels (Dong and Wu, 2007). The response activates intracellular response systems, but also activates a pathway to desensitize, endocytose, and down-regulate the activated GPCRs. Desensitization prevents overstimulation against prolonged agonist stimulation by tapering off the intracellular response to receptor activation. GPCR signaling is also regulated by internalizing and sequestering activated GPCRs into internal cellular compartments through endocytosis. Internalization occurs within seconds to minutes after agonist binding and once internalized, GPCRs are either

dephosphorylated (de-activated) and recycled as functional receptors to the cell membrane or are directed to lysosomes (Seachrist and Ferguson, 2003).

GnRHR

Hypothalamic hormones are part of an endocrine mechanism influenced by the central nervous system. The hypothalamus and pituitary create a link between neural and hormonal systems of the body. Gonadotropin-releasing hormone (GnRH) is released by the hypothalamus and travels via this closed portal system to the pituitary where GnRH binds to the gonadotropin-releasing hormone receptor (GnRHR) on the surface of gonadotrope cells. The GnRH receptor is a glycoprotein GPCR, and ligand-binding triggers receptor coupling with a G-protein and an intracellular response within gonadotropes. The signal cascade stimulates systemic release of varying levels of luteinizing hormone and follicle stimulating hormone that lead to secondary sex hormone production in the gonads. Intense GnRH release triggers ovulation through this endocrine system (Millar et al., 2004).

Like other GPCRs, upon agonist ligand-binding, the GnRH receptor couples to G-proteins G_q/G_{11} and has also been shown to couple with a number of other G-proteins based on availability (Hoffman et al., 2000). Once stimulation occurs, the G_q protein activates phospholipase C, which in turn cleaves phosphatidylinositol 4,5-bisphosphate into diacyl glycerol and inositol 1,4,5-triphosphate (IP_3). The IP_3 is released into the cytosol where it binds to receptors opening calcium channels in the endoplasmic reticulum, triggering an intracellular response. While other GPCRs are characterized by having carboxyl-termini within the cell, the GnRH receptor protein lacks a C-terminal tail protruding into the cytoplasm (Conn and Melmed, 1997, Hoffman et al., 2000).

Vesicular Trafficking

Vesicular trafficking is an organized and specific mechanism of transportation throughout the cell. Anterograde trafficking is defined as any action that moves vesicles from the endoplasmic reticulum through the ER-Golgi intermediate compartment to the *cis*-, medial and *trans*-Golgi network, and eventually to the cell membrane. Retrograde trafficking is the reversal of that pathway, including endocytosis and targeting to lysosomes for degradation. Vesicular trafficking allows a continuous exchange between membranous compartments and is essential for secretion, engulfment, and organelle biogenesis, but also the control of expression of GPCRs and other membrane-bound proteins (Alberts et al., 2008). GPCRs are translated in the endoplasmic reticulum and properly folded by chaperone proteins. Once folded, receptors are organized into ER-derived COPII transport vesicles. Vesicles carrying GPCRs are directed to the ER-Golgi intermediate complex. During the subsequent transport through the Golgi apparatus and *trans*-Golgi network, receptors become post-translationally modified through glycosylation to achieve mature status before being transported to the plasma membrane (Dong and Wu, 2007). The balance of intracellular traffic determines the level of receptor at the plasma membrane and influences the magnitude of cell response. Disruption of GPCR export trafficking causes many loss-of-function diseases as membrane expression drops (Duvernay et al., 2005).

Rab Proteins

Vesicular movement between membranes is guided by Rab GTPase proteins. Rab proteins are key directors in the formation, movement, tethering and fusion of vesicles. Rab proteins move by associating with myosin and traveling on actin filaments before binding to

Rab effector proteins and tethering via v-SNARE and t-SNARE interactions (Alberts et al., 2008). As members of the Ras family, GTPases cycle between an inactive GDP bound form and an active GTP bound form. The GDP/GTP exchange is catalyzed by the association of a guanine nucleotide exchange factor and hydrolysis is catalyzed by GTPase-activating proteins (Bhattacharya et al., 2004). Additionally, Rab proteins regulate vesicular protein transport through endocytosis and exocytosis, although Rab protein involvement is best understood in endocytosis (Duvernay et al., 2005). More than 63 distinct mammalian Rab GTPases have been characterized and although the proteins are ubiquitous and highly conserved, each Rab protein has a unique intracellular localization (Bhattacharya et al., 2004). Localizations and directional trafficking of Rab GTPases, as discovered in studies involving extremely diverse vesicular cargo, are listed in Table 1. This might serve as a foundation for further studies, but the diverse biochemical properties of vesicular cargo are hypothesized to cause specialized interactions with Rab proteins that direct trafficking; these recorded pathways are not necessarily conserved for all cell types and vesicular cargo. It is likely that many different Rab proteins compete to bind vesicles, with cell membrane expression controlled by desensitization and re-sensitization conditional upon the collection of Rab proteins expressed. Isoforms of these proteins occur frequently with similar properties and greater than 90% identity in amino acid sequence and are denoted by letters following the Rab number (Duvernay et al., 2005). Among differentiated cells, concentrations of specific Rab proteins vary greatly to meet the demands of the cell type. Vesicular cargo is a suspected factor that signals a Rab protein association with specific vesicles to organize movement appropriately.

Human Rab GTPases: Localization and Directional Trafficking

Rab Protein	Localization	Directional Trafficking
Rab1b	ER-Golgi, *cis*-Golgi	Anterograde
Rab2a	ER-Golgi, *cis*-Golgi	Retrograde
Rab3a	Synaptic vesicles, secretory granules, plasma membrane	Anterograde
Rab3b	Secretory granules, plasma membrane	Anterograde
Rab3c	Synaptic vesicles, plasma membrane	Anterograde
Rab3d	Secretory granules, plasma membrane	Anterograde
Rab6a	ER, Golgi, *trans*-Golgi network	Retrograde
Rab6c	No identified membrane localization	Retrograde
Rab7b	Late endosomes	Retrograde
Rab8a	*Trans*-Golgi network, secretory vesicles, plasma membrane	Anterograde
Rab9a	Late endosomes, *trans*-Golgi network	Retrograde
Rab9b	Late endosomes, trans-Golgi network	Retrograde
Rab10	*Trans*-Golgi network, basolateral sorting endosomes, GLUT4 vesicles	Anterograde
Rab11a	Recycling endosomes, *trans*-Golgi network, plasma membrane	Retrograde
Rab11b	Recycling endosomes, *trans*-Golgi network, plasma membrane	Retrograde

*Table 1.*Known membrane localization and directional trafficking of Rab GTPases studied. These properties were amassed in a review article by Hutagalung and Novick (2011). The studies that were compiled investigated Rab protein vesicular trafficking of a wide variety of cargo. This information is an important reference point, but cannot predict specific Rab GTPase interactions with chemically unrelated vesicular cargo. Data for Rab protein Rab6c came from Goud and Akhmanova (2012).

Previous studies have shown GPCRs interact with Rab GTPases. Lachance et al. 2011, demonstrated that the C-terminus region of the β-2 Adrenergic Receptor (a GPCR) interacted with both specific Rab proteins and Rab geranylgeranyltransferase in the anterograde travel from the ER to the cell membrane. It is believed that the mechanism of this process involves

post-translational modifications of the Rab proteins by geranylgeranlyation, a form of prenylation attaching geranylgeranyl moieties to cysteine residues. This step is essential for Rab proteins to closely associate with membranes (Seachrist and Ferguson, 2003). The GPCR C-terminus (which is fairly conserved among GPCRs) is used as a scaffold to modulate the geranylgeranylation step that activates Rab proteins with the aid of a Rab escort protein (Lachance et al., 2011). It has yet to be determined if this mechanism is conserved across all or most GPCRs or if it is specific to the β-2 Adrenergic Receptor used in the study. It is also possible that the lack of a C-terminus in GnRHR could affect this interaction. Also unknown is the role of oligomerization in the ER-Golgi complex during GPCR protein synthesis, although it is hypothesized that it regulates post-translational cell surface expression (Conn et al., 2007).

Defective Rab GTPase regulation manifests itself in several diseases. Griscelli syndrome is an autosomal dominant polycystic kidney disease caused by abnormal Rab function. X-linked choroidermia, and X-chromosome-linked mental retardation are both caused by genetic defects in Rab protein regulators. Dialated cardiomyopathy is a condition caused by increased Rab1 (a confirmed anterograde Rab protein) expression in the myocardium that leads to overexpression of the h_2AR and produces cardiac hypertrophy and eventual heart failure (Duvernay et al., 2005).

Structure-associated disease

Structure is essential to the function of the glycoprotein receptor, and non-conservative mutations can result in disease due to the failure to propagate the hormone response. Loss of function diseases are caused by one of three faults: 1) a binding site defect, 2) failure to couple to a G-protein, or 3) no surface expression of the receptor. Lack of surface expression is a much

more subtle defect, and can arise from: failure to integrate properly into the cellular membrane, inability to pass the rigorous examination of the quality control system in the ER, or as mentioned above, lacking scaffolding properties for associated Rab proteins (Hoffman et al., 2000). Each of these measures function as preventative measures to ensure proper folding, but when misfolded proteins are misrouted or accumulate to dangerously high levels, this can lead to apoptosis (Duvernay et al., 2005). Diseases caused by decreased or absent receptor expression due to the retention of misfolded or incompletely processed proteins include: Leydig cell hypoplasia, a rare male pseudohermaphroditism, ovarian dysgenesis, congenital hypothyroidism, familial hypocalciuric hypercalcemia reducing calcium-sensing receptor function, an inhibition of melanocortin-related receptor expression found in patients with morbid obesity, and interestingly, in subjects with resistance to human immunodeficiency virus infection. Diseases driven by aggregation include: retinis pigmentosa, caused by ER-trapping of mutant rhodopsin (a GPCR) and producing photoreceptor degeneration, nephrogenic diabetes where mutant vasopressin type 2 receptors cannot reach the plasma membrane and hypogonadotropic hypogonadism, a misfolding of the GnRH receptor causing misrouting and inexpression at the plasma membrane. Hypogonadotropic hypogonadism manifests as a failure of pituitary gonadotropes to interpret GnRH presence, resulting in lower or apulsatile gonadotropin release, with infertility in both males and females. Diagnosis is confirmed by low levels of luteinizing hormone despite giving high levels of GnRH. Due to the reproductive nature of the disease, it is not fatal, is usually undiagnosed, and mutations are not passed to offspring. About 90% of the GnRHR mutations that have been observed are trafficking-defective (Conn et al., 2007).

The human GnRH receptor is susceptible to misfolding due to a failure to form a sulfhydryl bridge from Cys^{14}-Cys^{200}, resulting in the quality control system retaining the protein in the endoplasmic reticulum. The bridge is essential only for primates that have a proximal Lys^{191} residue where rats and mice do not. Deletion of this residue from the primate sequence increases bridge formation and proper folding while the addition of Lys^{191} had no effect on plasma membrane expression. This suggests that lysine alone is not responsible for misfolding, and motifs were identified in multiple domains of the human receptor that negatively affect the ability to stabilize the sulfhydryl bridge in the presence of Lys^{191} (Janovick et al., 2006).

The less-efficient ligand binding affinity of GnRH in primate systems caused by the extra lysine is hypothesized to be evolved for more complex regulation of sex hormones. Rather than GnRH levels being very responsive to any change in GnRH presence, only high level stimulate cell response, generating a more regulated system. While this creates more likelihood of reproductive mutations, it has evolutionarily allowed animals with higher levels of metabolic investment and survival rates increased regulatory control of reproduction than animals with lower investment and survival rates—essentially limiting litter size and creating longer reproductive cycles (Janovick et al., 2006).

To increase the control of plasma membrane expression of GnRHR, the cell uses molecular chaperone proteins of the ER such as calnexin to retain functional proteins that are inactive while they are misfolded, but could quickly be folded and escorted to the plasma membrane for rapid availability. The misfolded GnRHR proteins have been rescued both *in vitro* and in mice (with human-like GnRHR mutations) by small, hydrophobic chemical compounds acting as chaperones (pharmocoperones) allowing the GnRHR to escape the ER quality control

system and route properly (Janovick et al., 2013). Similar retention of other GPCRs suggests that restricted trafficking is a more common regulation mechanism than previously believed. It is hypothesized that mutations have a proportionally larger effect on smaller GPCRs such as GnRHR and as such, are more frequently affected by mutations causing ER retention and disease. As misfolds are much more sensitive in smaller GPCRs, they are more likely to be rescuable by pharmocoperones that can overcome thermodynamics favoring alternative formations (Conn et al., 2007).

III. EXPERIMENTAL PROCEDURE

DNA Amplification

Rab protein DNA plasmids containing ampicillin or kanamycin resistant markers (see Appendix 1) were obtained from an external lab. Many of these samples were modified with affinity tags using recombinant DNA technology. The FLAG-tag is a polypeptide tag used for antibody assays, GFP-tag is used for fluorescent tagging of proteins, HA-tag (hemagglutinin) aids detection of the tagged protein, WT indicates a wild-type protein and NI indicates the substitution of an asparagine at amino acid 119 to isoleucine. Mutant alleles (Rab11aN124I-flag and GFP-Rab2N119I) are dominant-negative, blocking normal retrograde trafficking pathways of Rab11a and Rab2, respectively. If the wild-type Rab GTPases are indeed retrograde traffickers of GnRHR, higher levels of receptor expression should be present with mutated versions than wild-type.

Plasmids containing Rab protein DNA were transformed into 50 µL *E. coli* cells on ice for 2 min, then 42 ˚C water bath 1 min before plated onto respective antibiotic-treated agar plates

incubated at 37 ˚C overnight. A colony was isolated aseptically and added to 5 mL LB medium, 5 µL 50 mg/mL ampicillin (or kanamycin) in 50 mL tubes. Tubes were mixed at 205 rpm for six hours. The bacterial solution was added aseptically to 250 mL LB medium, 250 µL 50 mg/mL ampicillin (or kanamycin) in Erlenmeyer flask. Flasks were mixed at 160 rpm for 15 hours at 37 ˚C in water bath. A maxi-prep to extract DNA was performed using a Qiagen EndoFree Plasmid Purification kit (Valencia, California) according to the instructions. Original dilutions of DNA concentration in EndoFree TE buffer were analyzed using a spectrometer that measured absorbance at wavelengths 260 µm, 280 µm and 320 µm.

An enzyme digest was done for each Rab plasmid sample using known sequences in the antibiotic resistance genes for restriction sites, and leaving the Rab sequence. To 0.5 µL of each DNA sample, 15 µL milli-Q water was added. Each diluted sample then received 0.5 µL 10 mg/mL (100X) bovine serum albumin (20 mM Tris-HCL, 100 mM KCl, 0.1 mM EDTA, 50% glycerol with pH 8.0 at room temperature from the New England Biolabs, Ipswich, Massachusetts NEBuffer Set 1, 2, 3, 4 & BSA). To ampicillin-resistant samples, 2 µL NEBuffer #2 composed of 50 mM NaCl, 10 mM Tris-HCl, 10 mM $MgCl_2$, 1 mM DTT with pH 7.9 at room temperature) was added followed by 20 units *HindIII* and 20 units *XhoI*. To kanamycin-resistant samples, 2 µL multicore buffer (New England Biolabs) was added, followed by 10 units *KpnI* and 50 units *ApaI*. Aliquots were mixed, then spun in a centrifuge for 2 seconds to bring all liquid to the bottom. Samples were incubated at room temperature for 2 hours. A 1% agarose gel was prepared with SYBR Safe. Post-incubation, 2 µL loading DNA dye was added to each sample. To the first two wells, 3 µL 1000 bp and 100 bp ladders were loaded, respectively. The prepared samples were mixed before loading into wells. Gel electrophoresis was allowed to run at 90 V

for 90 minutes. Gels were imaged and size (in base pairs) was compared to known length of Rab DNA (Appendix 3) to confirm Rab sequence (RCSD Protein Data Bank).

Cell Culture Propagation and Plating of cells

Cos-7 African green monkey kidney tumor cells were allowed to grow in Dulbecco's Modified Eagle Medium (DMEM)/10% Fetal Calf Serum (FCS)/Gentamicin (DFG) inside a CO_2 regulating chamber at 37 ˚C. Propagation of these cells was maintained prior to experimentation by thinning cells twice a week to 3 million per flask. Prior to use, 100 mL DFG, 25 mL 1X PBS was warmed to 37 ˚C. All cell work took place within a sterile hood.

Flasks containing cells were emptied of all DFG and quickly washed with 25 mL PBS, poured down the side opposite to the cells before being allowed to gently wash cells. To the flask, 5 mL Trypsin/EDTA was added, and the solution was swirled over cells. The flask was placed back into the incubator at 37 ˚C for 3-5 minutes. The flask was removed and the sides of the container were hit gently to knock cells loose. In the hood, flask was emptied into a 50 mL sterile tube containing 15 mL DFG. Flask was rinsed with 30 mL DFG, poured into a 50 mL tube and was centrifuged at 750 rpm for 10 minutes. The supernatant was discarded and the pellet resuspended in 750 µL DFG and mixed gently with a pipet 15 times. To this mixture, 5 mL DFG was added and solution was mixed 6 times. A 1:20 dilution of cells was made (950 µL DFG, 50 µL cell solution) and 10 µL of the solution was loaded into each side of a hemocytometer. Cells were counted under a light microscope to determine cell concentration. To the flask, 3 million cells were returned and placed back in the incubator at 37 ˚C for 20-24 hours.

For the experiment, cell solution was diluted to 50,000 cells/250 µL and 250 µL of this solution was pipetted into each well in 48-well plates, with 4 wells plated for each anticipated treatment.

Cell Transfection and Changing Medium

Using standard DNA concentrations (ng/µL), calculations were performed to ensure equal quantities of Rab DNA were added to each sample. Milli-Q water was added to maintain equal amounts of solution were added to each well. Appendix 4 shows the composition of each transfection sample. After 20 hours of incubation, cells were checked for contamination and OPTI-MEM reduced serum culture media (Life Technologies, Carlsbad, California) measured out and warmed to 37 ˚C in water bath. In the sterile hood, milli-Q water was added to aliquots based on calculations (Appendix 4). To each aliquot, 23.62 µL OPTI-MEM was pipetted, followed by hGnRHR (according to Appendix 4). Vector was added to the respective aliquots, and each Rab DNA sample was added according to calculations. To separate 1.5 mL aliquots (1 per treatment), 4.5 µL Lipofectamine was added, followed by 22.5 µL OPTI-MEM. Each DNA solution was mixed, then pipetted into the Lipofectamine solution and mixed gently with pipet 7 times. Samples were moved every 30 seconds to ensure all solutions were incubated exactly 45 minutes at room temperature.

After 35 minutes, the 48-well plates were dumped and blotted twice. To each well, 0.5 mL OPTI-MEM was added. All wells were filled within 4 minutes of each dumping so cells did not dry out. After 45 minutes, 513 µL OPTI-MEM was added to each sample and tube was mixed by gently inverting 10 times. The well plates were dumped and blotted twice, and 125 µL of DNA solution from the tubes was added to each well. The well plates were incubated at 37 ˚C

for exactly 5 hours after the time DNA was added to the first well of each plate. Immediately after completing transfection, 20% FCS solution was prepared with 3.2 mL FCS added to 12.8 mL DMEM in a bottle. This was placed in the water bath for later usage. After exactly 5 hours of incubation, 125 µL 20% FCS was added to each well. Cell plates were returned to the incubator at 37 ˚C for 18 hours.

After 18 hours of incubation, DFG, DBG (minimal culture medium), and inositol-free synthetic medium (IFM) were measured and warmed to 37 ˚C in water bath. Contents of wells were dumped and well plates were blotted twice, before 250 µL DFG was added to each well. Well plates were returned to incubator at 37 ˚C for 4 hours. After 4 hours incubation, wells were again dumped and blotted twice. To each well, 0.5 mL DBG was added. This wash was repeated twice leaving the final DBG wash on the cells. To 30 mL IFM, 120 µL tritium inositol was added. To each well, 250 µL IFM with 4 µCi/mL ^{3}H-inositol was added. Well plates were returned to incubator at 37 ˚C for 18 hours.

Stimulation of Cells and Radioimmunoassay of Overall Inositol Phosphate Production

After 18 hours of incubation, IFM was warmed to 37 ˚C in water bath. 0.0223 g LiCl (a phospholipase-C inhibitor) was dissolved in 105 mL IFM to create a 5 mM LiCl solution. Cell plates were dumped, blotted twice, and then re-filled with 300 µL IFM. Cell plates were washed in this manner two times. To 35 mL IFM with LiCl, 3.5 µg Buserelin (a GnRHR stimulator) was added, resulting in a 0.1 µg/mL Buserelin concentration. Well plates were dumped, blotted twice, and to each well 250 µL IFM/LiCl/Buserelin was added. Well plates were returned to incubator at 37 ˚C for 2 hours. After two hours, well plates were dumped, blotted twice, and to

each well 500 µL 0.1M formic acid was added. Plates were sandwiched between sheets of dry ice until all wells were frozen and then thawed in a shallow water bath.

Four rows of test tubes were arranged for each sample. Ion exchange columns were fashioned for each well with 600 µL Dowex in each column. Columns were washed with 3 mL 0.1M formic acid to equilibrate the column. To each well, 500 µL 0.1M formic acid was added to rinse, and well contents were pipetted into the respective columns. To each column, 2 mL 0.1M formic acid was added, and allowed to drip through completely. Columns were moved to the third row of test tubes and to each column 3 mL 0.1M formic acid was added, and allowed to drip through completely. Columns were moved to the final row of tubes and eluted with 3 mL 1M ammonium formate/0.1M formic acid. Once columns had dripped to completion, tubes were gently vortexed to mix.

From each tube, 500 µL solution was pipetted into a respective scintillation vial. To each vial, 4.5 mL Bio-Safe II scintillation cocktail was added and vials were capped. Radioactivity was measured in counts per minute (cpm). Radioactivity demonstrated the presence of inositol phosphates in the samples, and activity of the Rab proteins was assessed relative to a control that contained no Rab protein.

IV. RESULTS

DNA Amplification

Rab protein plasmid transformation into *E. coli* cells was successful for all samples, as colonies grew on ampicillin or kanamycin (Appendix 1), confirming Rab protein insert presence in the bacterial DNA. After DNA extraction, original dilutions of extracted DNA were measured

using a spectrophotometer. The proportion of absorbance at 260 µm/280 µm is indicative of protein concentration, with a desired ratio being between 1.7 and 2.0 (to avoid too few or too many proteins). All samples fell in this range. Absorbance at 260 µm was used to calculate DNA

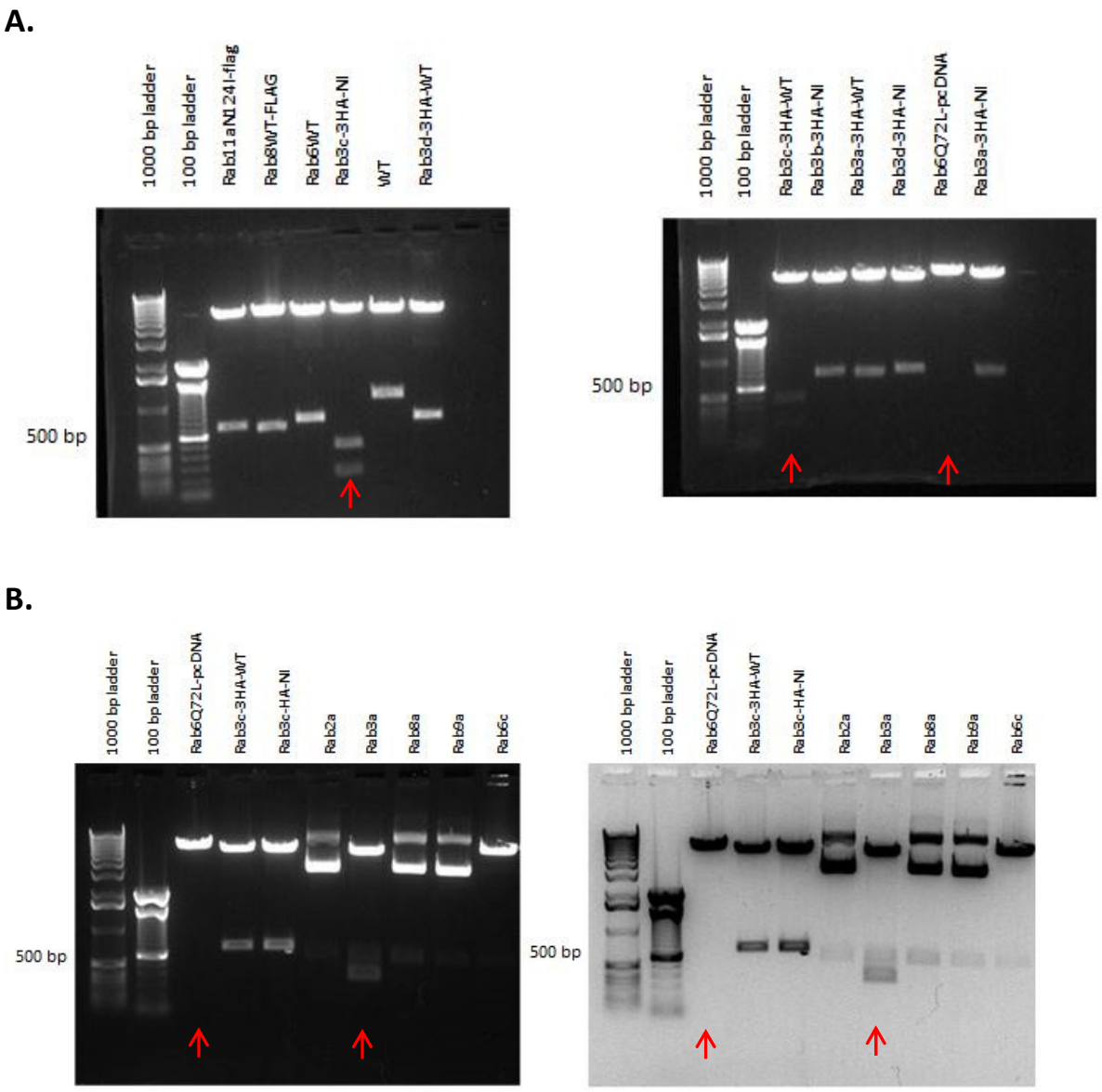

Fig. 1. Enzyme digestion followed by gel electrophoresis confirms Rab protein insert presence in DNA. Plasmids in Fig1A were digested with *HindIII* and *XhoI*, while all samples in Fig1B were digested by *KpnI* and *ApaI* except Rab6Q72L-pcDNA (*HindIII* and *XhoI*) and samples Rab3c-HA-WT and Rab3c-HA-NI (both *BamhI* and *XhoI*). Known lengths of Rab genes are between ~600 and 750 bp. Unpredicted outcomes are marked with red arrows. A. Expected bands indicate Rab gene insert is present in all samples except Rab6Q72L-pcDNA and Rab3c-3HA-WT. There are two bands occurring where only one should occur for Rab3c-3HA-NI. B. The image and inverted image show Rab protein insert is present in all except Rab6Q72L-pcDNA second trial. Rab3a shows two bands. Rab3c-HA-WT and Rab3c-HA-NI were submitted to a different enzyme digest and re-run through gel electrophoresis, confirming Rab protein insert was present.

concentration in ng/µL. For samples GFP-Rab2WT, GFP-Rab2N119I, Rab2a, Rab3a, Rab8a, Rab9a, Rab10, Rab11a, Rab6c, Rab7b, Rab8b, Rab9b raw and adjusted absorbance levels were much lower than the rest of the Rab DNA concentrations (Appendix 2). The DNA/protein ratio was still within usable range but DNA concentration was roughly 10% of the other samples.

Enzyme Digest and Gel Electrophoresis

All reported Rab GTPase DNA insert lengths that were used in this study fell between ~600 and 750 base pairs. Figures 1A, 1B, 2A, 2B, and 2C depict annotated photographs of Rab GTPase DNA inserts digested and run on gels. In Figure 1A, bands can be seen in the anticipated range for Rab DNA, confirming the presence of the Rab protein insert (except those marked with red arrows). Rab6Q72L-pcDNA and Rab3c-3HA-WT do not show any small bands of DNA where the insert should be. Rab3c-3HA-NI has two bands with both bands slightly smaller in size than the anticipated insert signal. The Rab3c DNA sequence had a *HindIII* restriction site within the coding region, so the enzyme digest was performed again for both Rab3c-3HA-WT and Rab3c-3HA-NI samples with Buffer #2, *XhoI* and *BamhI* to ensure the entire Rab3c sequence was present. The same enzyme digests and gel electrophoresis was repeated for Rab6Q72L-pcDNA. Figure 1B shows the results of this second trial and both Rab3c-3HA-WT and Rab3c-3HA-NI showed single bands. Rab6Q72L-pcDNA shows no Rab protein insert present again, and Rab3a shows two bands. Figure 2 shows Rab protein inserts present in all proteins, and re-test of Rab3a sample once again shows two bands. Moving forward into transfection, all samples were used despite confirmation of Rab protein insert presence.

A.

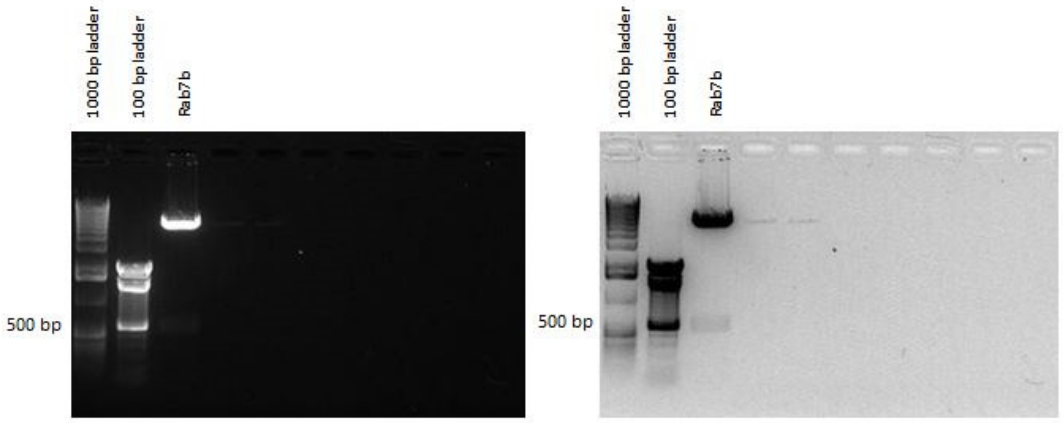

B.

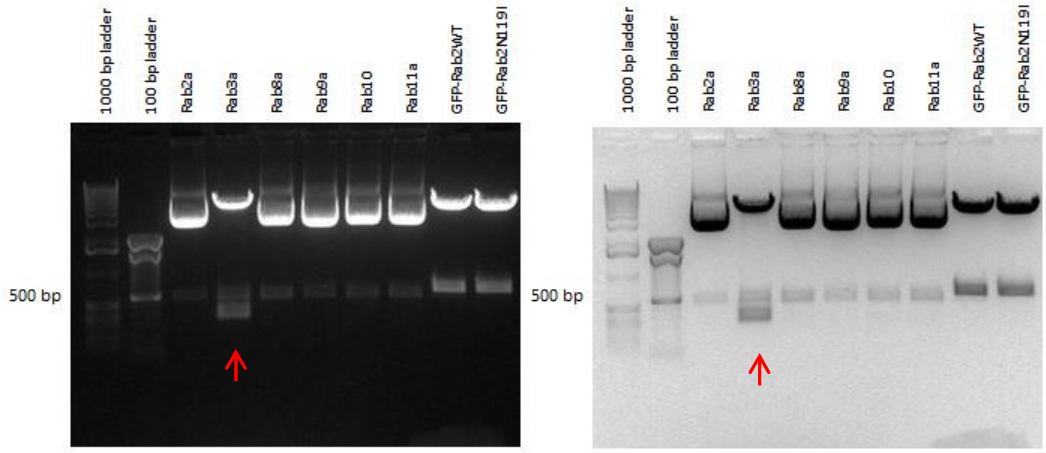

C.

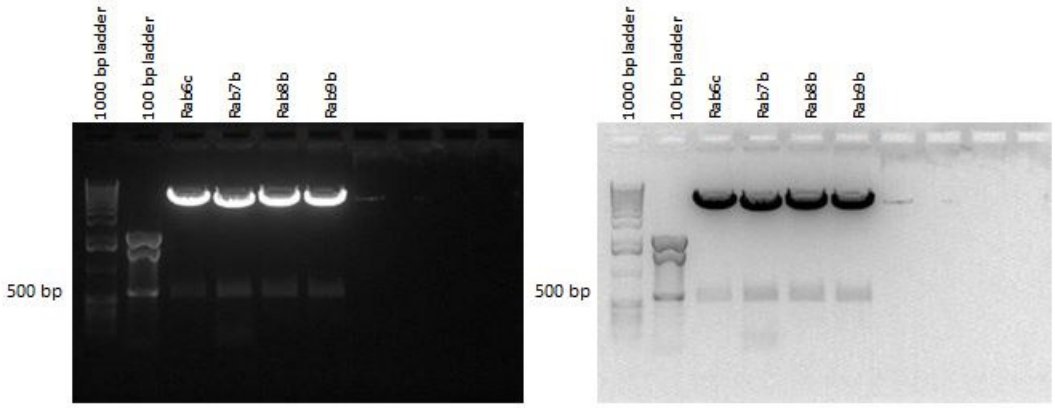

Fig. 2. Enzyme digestion by *KpnI* and *ApaI* followed by gel electrophoresis confirms Rab insert presence in DNA. Known lengths of Rab sequences are between ~600 and 750 bp. Unpredicted outcomes are marked with red arrows. Initial imaging and inverted images are shown. A. Rab7b sample is confirmed to have insert present in DNA. B. All samples have Rab insert present, with Rab3a again showing two bands. C. All samples contain Rab insert.

Radioimmunoassay of Overall Inositol Phosphate Production

Cos-7 African green monkey kidney tumor cells were transfected with equal parts (DNA concentrations taken into consideration) of Rab DNA and equal amounts of human wild-type GnRH receptor (hWT GnRH) DNA. Inositol phosphate (IP) is produced in a signal cascade upon GnRH receptor stimulation. Total IP counts are relative to the level of intracellular response, and are representative of GnRH receptor expression at the cell membrane. Total IP levels were measured by radioactivity counts (counts per minute) of each sample.

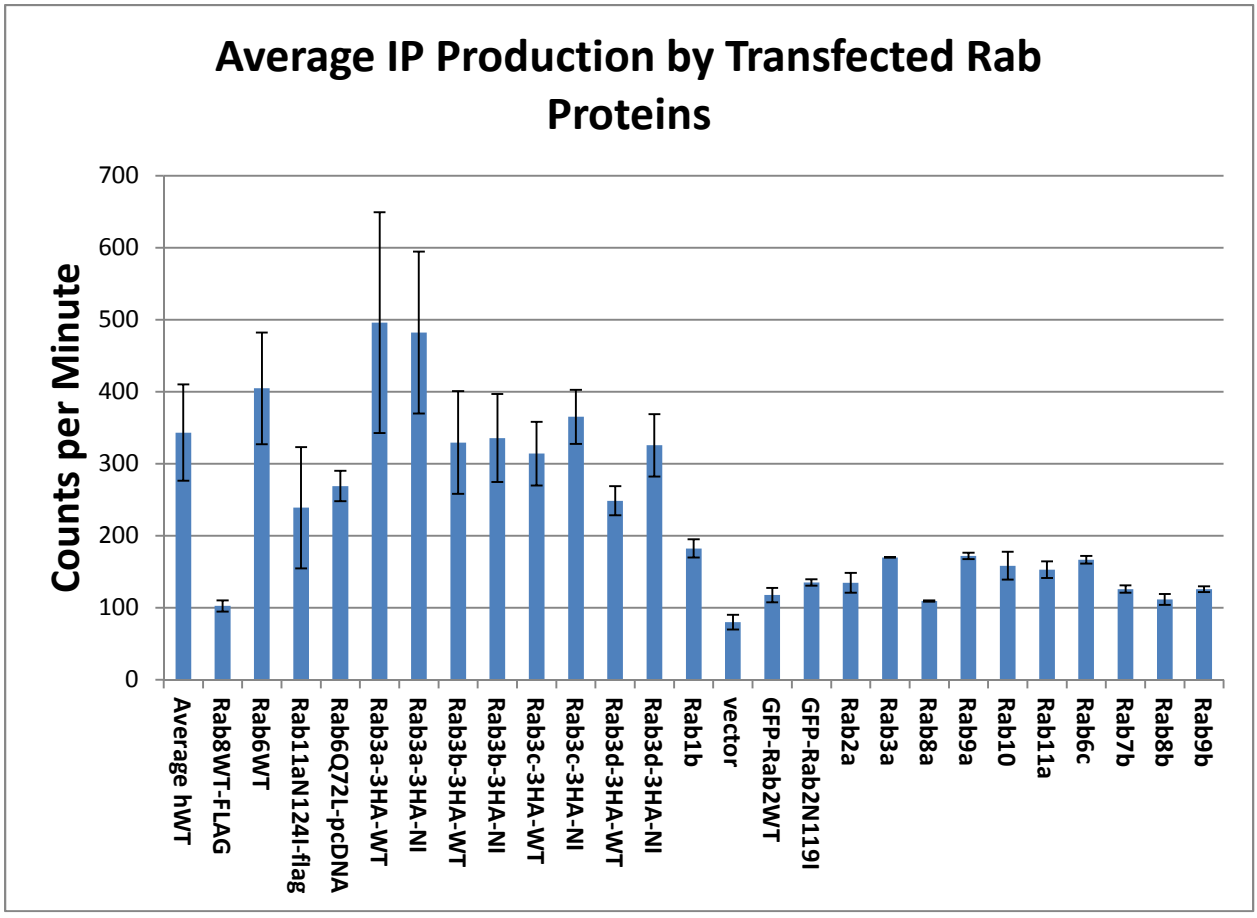

Fig.3. Average total IP production for each Rab protein sample. Radioactive counts per minute are relative to the total inositol phosphate production by cells. In turn, IP production is dependent on presence of GnRH receptor at the cell membrane.

Due to the experimental timeline, three trials were performed for some samples and only two trials were performed for the remainder of the samples. The transfection with only human wild-type GnRH receptor and vector averaged a 343 cpm (counts per minute) output with a standard error of 67. Figure 3 graphs the average radioactivity count (in cpm) for each sample, with the far left bar being the hWT GnRH receptor control. This acted as a control output that all IP production was compared against to effectively view the impact of the specific Rab protein on amount of GnRH receptor at the plasma membrane. The vector also acts as a control to view cpm output where no hWT GnRH or Rab proteins were added.

Relative to the control, three proteins produced a larger total cpm output (Figure 4). Rab6WT, Rab3a-3HA-WT and Rab3a-3HA-NI have outputs that are on average 18%, 40% and 44% of the control output. While this is notable, when standard error is considered, none of these samples can be defined as statistically larger than the control. Rab3c-3HA-NI has a 6.4% higher cpm than the control, but falls almost completely within the range of the standard error of the control. As anticipated, the vector control cpm is significantly lower than the hWT GnRH receptor control. Rab6WT-FLAG and Rab1b also show a statistically lower cpm production than the control. Rab11aN124I-flag, Rab6Q72L-pcDNA, Rab3b-3HA-WT, Rab3b-3HA-NI, Rab3c-3HA-WT, Rab3d-3HA-WT and Rab3d-3HA-NI all have very similar cpm outputs as the control but with varying degree of error. Mutants Rab11aN124I-flag and Rab2N119I both had higher total inositol phosphate production than their wild-type counterparts, but these difference were not statistically significant.

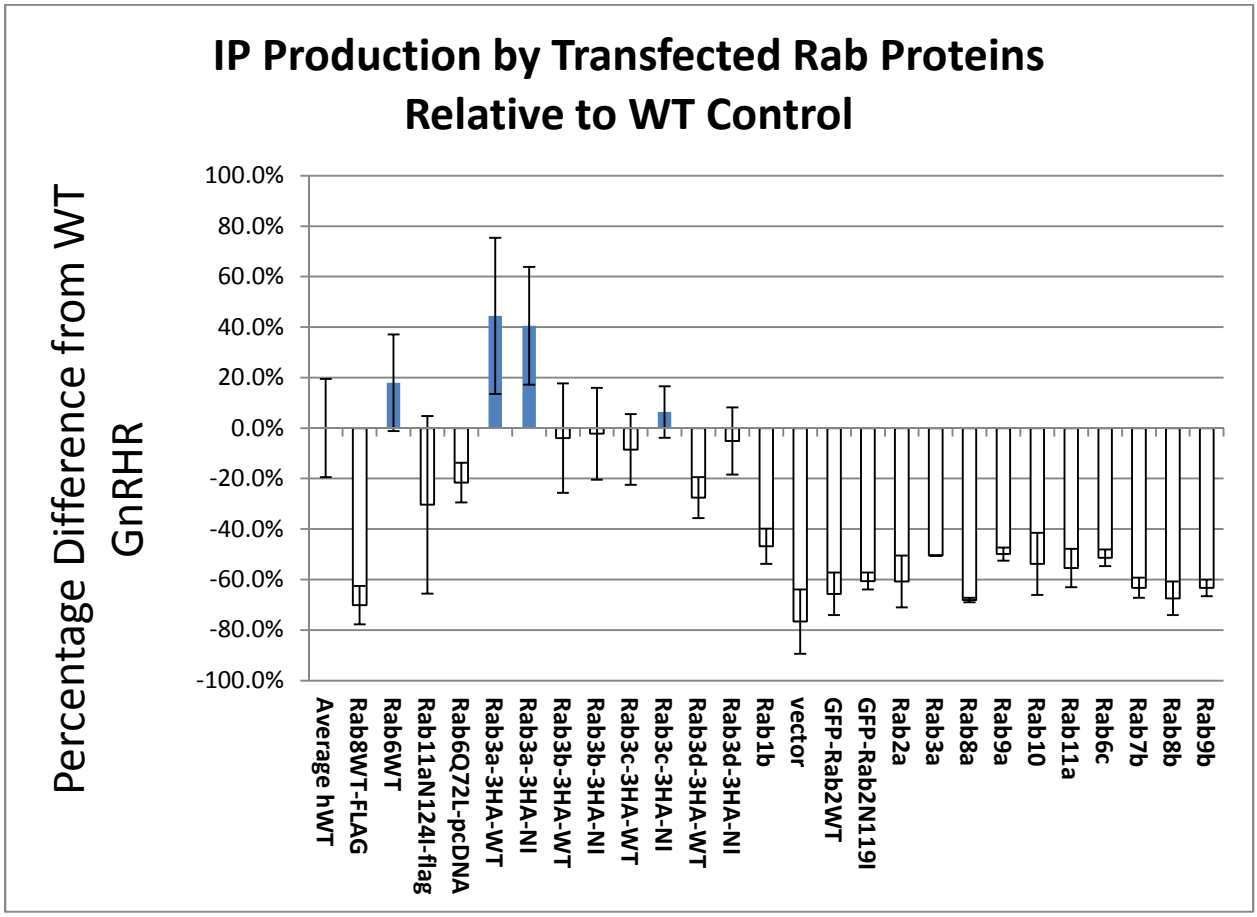

Fig. 4. Change in total inositol phosphate (IP) production by individual Rab proteins compared to control. Total (IP) production by cells containing Rab proteins co-transfected with human wild-type gonadotropin-releasing hormone receptor (hWT GnRHR) is graphed as a percentage of total (IP) production by cells only transfected with hWT GnRHR. Markedly increased IP production indicates potential anterograde properties while decreased IP production indicates likely retrograde actions. IP production similar to hWT GnRHR is inconclusive or indicates that the specific Rab protein is inactive in hWT GnRHR trafficking.

Curiously, all of the samples that had significantly less concentrated DNA in the spectral analysis resulted in much lower cpm outputs than the control. GFP-Rab2WT, GFP-Rab2N119I, Rab2a, Rab3a, Rab8a, Rab9a, Rab10, Rab11a, Rab6c, Rab7b, Rab8b, and Rab9a all have statistically lower cpm outputs than the control and all samples have relatively small standard errors. These Rab GTPases were all in kanamycin-resistant plasmids, while the Rab proteins

with higher radioactivity counts were in ampicillin-resistant plasmids. It is likely that the expression vectors in the kanamycin-resistant plasmids had a much lower copy level.

V. DISCUSSION

Interpreting the Data

To determine whether a Rab protein was responsible for anterograde or retrograde trafficking or had no influence, GnRH receptor presence at the cell membrane was recorded indirectly using the total radioactivity of newly synthesized (upon ligand stimulation of receptor) inositol phosphates (IPs) in each sample as a determinant. Interpretation of the radioactive inositol phosphate presence was in relation to the amount of IPs occurring in transfections of human wild-type GnRH receptor DNA and no additional Rab GTPase DNA. It was found that Rab6WT, Rab3a-3HA-WT and Rab3a-3HA-NI (a mutation expected to behave similarly to the wild-type), caused an increase of GnRH receptor expression, suggesting these proteins are active in the anterograde process. The degree of variance in the data does not statistically allow us to correlate these proteins as anterograde, but the experimental design of this project is only to indicate proteins of interest for further exploration of anterograde properties. Rab proteins Rab8WT-FLAG and Rab1b had significantly lower IP levels than the control, and are very likely retrograde traffickers of GnRH receptors. Proteins Rab11aN124I-flag, Rab6Q72L-pcDNA, Rab3b-3HA-WT, Rab3b-3HA-NI, Rab3c-3HA-WT, Rab3c-3HA-NI, Rab3d-3HA-WT, and Rab3d-3HA-NI all had receptor expression levels, based on IP levels, that were very statistically similar to the control and thus will require further experimentation to reveal the anterograde, retrograde or non-participatory natures of each.

All other proteins: GFP-Rab2WT, GFP-Rab2N119I, Rab2a, Rab3a, Rab8a, Rab9a, Rab10, Rab11a, Rab6c, Rab7b, Rab8b, and Rab9b all had significantly lower radioactive IP outputs than the control and also had much less variation between trials. All of these samples came from transfected DNA that was amplified and purified at the same time. During measurements determining dilutions of purified DNA, these samples were ten times less concentrated than the other grouping of proteins. This difference was accounted for in the dilutions of DNA for transfections, but the almost uniformly low IP counts suggest experimental error in these samples. As these erroneous samples were transfected using carefully calculated dilutions and using the same procedure during the same time period, it is most likely that this error comes from the kanamycin-resistant plasmids having a lower DNA copying rate than the ampicillin-resistant plasmids.

Dominant-negative mutants blocking normal trafficking of Rab11a and Rab2 were used to support evidence of directional vesicular movement by these wild-type Rab GTPases. Both Rab11a and Rab2 are thought to be involved with retrograde trafficking, and mutants GFP-Rab2N119I and Rab11aN124I-flag showed slightly higher receptor expression levels (based on total IP counts) than the wild-type counterparts. This is expected, as the mutants impede the function of the respective Rab proteins in the retrograde pathway, allowing for a higher accumulation of the receptors at the plasma membrane, relative to the wild-type. This data is not statistically significant, and it is likely that receptor expression cannot be compared across Rab11a samples as the plasmids encoding the two DNA inserts have varying DNA copying rates.

Comparative Analysis of Results

When these results are compared to existing studies of Rab GTPase trafficking (Table 1), almost all of the directional vesicular trafficking matched. Even as mechanisms for transport vary with specific cargo, it is likely that as a whole the Rab trafficking system is conserved. Proteins Rab1b, Rab6a, Rab8a and Rab10 all had unanticipated effects on plasma membrane expression of GnRH receptor. Rab1b had a very strong, significantly lower receptor expression than the wild-type (indicating retrograde activity) while in Garcia et al. 2011, Rab1b association with COPII complexes in yeast cells implicated Rab1b as an anterograde trafficker. Rab6WT transfected cells presented with an increase in receptor membrane presence, while Dong and Wu 2007, studied other GPCR trafficking of α_{2B}-adrenergic, β_2-AR and angiotension II type 1 receptors and showed Rab6 to be involved in retrograde transport. It is also notable that the Rab6 wild-type increased receptor expression at the membrane while a mutated version (Rab6Q72L-pcDNA) caused decreased expression. Rab8a was part of a trial group that had much lower receptor membrane presence than the control, and was interpreted as retrograde despite Huber et al. 1993, showing anterograde activity of Rab8a in association with vesicular stomatitis virus-glycoprotein. Rab10 was also part of the group where experimental error is thought to have occurred. Levels of receptor presence indicate retrograde behavior, but English and Voeltz 2013, showed Rab10 to be an anterograde trafficker. The change in directional activities for Rab8a and Rab10 are likely due to experimental error. It is possible that Rab1b and Rab6WT differences were also caused by experimental error, but these changes in receptor expression, especially Rab6 greatly increasing receptor presence, could indicate interactions between Rab proteins and specific GPCRs.

Future Experimentation

This experiment is a small part of a much bigger project. With more than 63 distinct Rab proteins, and many more isoforms, this particular study served as a shotgun approach to identify Rab proteins of interest in the trafficking of human GnRH receptor to the plasma membrane. Due to time constraints, only 11 different distinct Rab proteins were tested with 14 isoforms comprising the remainder of the samples. While many more Rab proteins will need to be assessed, moving forward, we can eliminate proteins that reduced plasma membrane presence of GnRHR and further test samples that increased or had no conclusive effect on membrane expression. As the next step of anterograde trafficking protein activity analysis, cAMP production will be measured during receptor-ligand stimulation. Additionally, radioligand binding assays will be performed to assess binding affinities of expressed receptors. Once Rab proteins involved in anterograde trafficking for this GPCR have been identified, localization of the action of the different proteins can be determined by immunoblotting to measure association of Rabs with different maturity GnRH receptors and immunofluorescent GFP-tagging.

Therapeutic Potential

Understanding how specific Rab proteins control vesicular trafficking of GnRH receptors is beneficial to designing and implementing pharmaceutical treatment of hypogonadotropic hypogonadism (HH). Human GnRH receptor expression is limited biologically to better regulate number of offspring through a misfold in the receptor that inhibits trafficking to the plasma membrane, but is still functional. By increasing anterograde Rab protein expression, the amount of GnRH receptor presence in gonadotrope cells is increased as the functional but

slightly misfolded proteins are escorted at a higher rate to the plasma membrane. In many cases of HH where GnRH receptors are improperly targeted or retained, the likelihood of normal gonadotrope hormone production can be elevated for the duration of the time the individual seeks to procreate. Conversely, overexpression of retrograde Rab proteins active in endocytosis or trafficking to lysosomes could be utilized as a form of contraception.

Pharmocoperones have been developed to retrieve misfolded receptors to their normal state, increase membrane expression, and rescue the normal phenotype. This method is almost impossible to implement therapeutically as the pharmocoperones necessitate removal from the receptor upon membrane expression before gonadotropin-releasing hormone can bind. Therapeutic practices utilizing Rab protein expression are still hypothetical, but potentials for implementable pharmaceutical administrations are much more plausible as up-regulation and down-regulation of the Rab protein intermediates would not require pulsatile doses.

The knowledge of Rab protein trafficking mechanisms has implications beyond GnRH receptor expression. Many loss-of-function diseases stem from overexpression and under-expression of GPCRs due to ineffective transportation of the proteins. Because GnRH receptor expression levels have non-lethal impacts on the host, it is a preferential model of which to base research on. As GPCRs are highly conserved, Rab protein involvement could likely be derived from the GnRH model.

Conclusion

In this study, a number of distinct Rab proteins and isoforms were identified as probable candidates for trafficking gonadotropin-releasing hormone receptors to the plasma membrane. Moving forward, the properties of these Rab proteins will be further analyzed to assess the

mechanism of GnRH receptor expression at the cell membrane. Better understanding of Rab protein trafficking may provide therapeutic treatments for a large number of loss-of-function diseases related to GPCR expression by use of pharmaceutical manipulation of anterograde and retrograde Rab proteins.

VI. ACKNOWLEDGEMENTS

Thank you to Dr. P. Michael Conn for accepting me into his lab, assisting in the design of my experiment, and helping me to understand the concepts behind the experiment. I would like to acknowledge Jody Janovick for her training in essential lab techniques and daily supervision and guidance. Diana Gordon organized the summer internship program that I worked through. Oregon Health and Science University's (OHSU) Oregon National Primate Research Center (ONPRC) provided the laboratory venue. The Silver Family Foundation provided the finances needed for my internship program and the National Institute of Health funded lab costs for the larger project that my project was a part of. Dr. Ralph Bertrand was my primary reader and was my on-campus representative at Colorado College for recognizing off-campus research. Thanks as well to Dr. Darrell Killian, my second reader at Colorado College.

VII. REFERENCES

Alberts B, Johnson A, Lewis J, Raff M, Roberts K, Walter P (2008) Molecular Biology of the Cell. Fifth Edition. *Garland Science*, Taylor & Francis Group LLC, New York, New York:749-763.

Ballesteros J, Kitanovic S, Guarnieri F, Davies P, Fromme BJ, Konvicka K, Chi L, Millar RP, Davidson JS, Weinstein H, Sealfron SC (1998) Functional microdomains in G-protein coupled receptors. The conserved arginine-cage motif in the gonadotropin-releasing hormone receptor. *J Biol Chem* **273:**10445-10453.

Bhattacharya M, Babwah AV, Ferguson SSG (2004) Small GTP-binding protein-coupled receptors. *Biochem Soc Trans* **32:**1040-1044.

Conn PM, Melmed S (1997) Endocrinology: Basic and Clinical Principles. *Humana Press*,

Totowa, New Jersey:185-191.

Conn PM, Ulloa-Aguirre A, Ito J, Janovick JA (2007) G protein-coupled receptor trafficking in health and disease: lessons learned to prepare for therapeutic mutant rescue *in vivo*. *Pharmacol Rev* **59:**225-250.

Cui J, Smith RG, Mount GR, Lo R-L, Yu J, Walsh Tf, Singh SB, DeVita RJ, Goulet MT, Schaeffer JM, et al. (2000) Identification of Phe^{313} of the gonadotropin-releasing hormone (GnRH) receptor as a site critical for the binding of nonpeptide GnRH antagonists. *Mol Endocrinol* **14:**671-681.

Dong C, Wu G (2007) Regulation of anterograde transport of adrenergic and angiotensin II receptors by Rab2 and Rab6 GTPases. *Cell Signal* **19:**2388-2399.

Duvernay MT, Filipeanu CM, Wu G (2005) The regulatory mechanisms of export trafficking of G protein-coupled receptors. *Cell Signal* **17:**1457-1465.

English AR, Voeltz GK (2013) Rab10 GTPase regulates ER dynamics and morphology. *Nat Cell Bio* **15(2):**169-178.

Garcia IA, Martinez HE, Alvarez C (2011) Rab1b regulates COPI and COPII dynamics in mammalian cells. *Cellular Logistics* **1(4):**159-163.

Goud B, Akhmanova A (2012) Rab6 GTPase. In Li G, Segev N (Ed.), *Rab GTPases and Membrane Trafficking*. *Bentham e-Books,* Oak Park, Illinois:34-46.

Hoffman SH, ter Laak TT, Kuhne R, Reilander H, Beckers T (2000) Residues within transmembrane helices 2 and 5 of the human gonadotropin-releasing hormone receptor contribute to agonist and antagonist binding. *Mol Endocrinol* **14:**1099-1115.

Huber LA, Pimplikar S, Parton RG, Virta H, Zerial M, Simons K (1993) Rab8, a small GTPase

involved in vesicular traffic between the TGN and the basolateral plasma membrane. *J Cell Bio* **123(1):**35-45.

Hutagalung AH, Novick PJ (2011) Role of Rab GTPases in Membrane Traffic and Cell Physiology. *Physiol Rev* **91(1):**119-149.

Janovick JA, Knollman PE, Brothers SP, Ayala-Yanez R, Aziz AS, and Conn PM (2006) Regulation of G protein-coupled receptor trafficking by inefficient plasma membrane expression: molecular basis of an evolved strategy. *J Biol Chem* **281:**8417-8425.

Janovick JA, Stewart MD, Jacob D, Martin LD, Deng JM, Stewart CA, Wang Y, Cornea A, Chavali L, Lopez S, Mitalipov S, Kang E, Lee HS, Manna PR, Stocco D, Behringer RR, Conn PM (2013) Restoration of gonadal function in hypogonadotropic hypogonadal mice by pharmacoperone drug therapy. *Proc Natl Acad Sci USA* **110(52):**21030-5.

Lachance V, Cartier A, Génier S, Munger S, Germain P, Labrecque P, Parent JL (2011) Regulation of β_2-adrenergic receptor maturation and anterograde trafficking by an interaction with rab geranylgeranyltransferase: modulation of rab geranylgeranylation by the receptor. *J Biol Chem* **286(47)**:40802-40813.

Millar RP, Lu ZL, Pawson AJ, Flanagan CA, Morgan K, Maudsley SR (2004) Gonadotropin-releasing hormone receptors. *Endocr Rev* **25(2):**235-275.

Seachrist JL, Ferguson SSG (2003) Regulation of G protein-coupled receptor endocytosis and trafficking by rab GTPases. *Life Sci* **74:**225-235.

VIII. APPENDICES:

Rab Protein gene in plasmid	Antibiotic Resistance
Rab8WT-FLAG	Ampicillin
Rab6WT	Ampicillin
Rab11aN124I-flag	Ampicillin
Rab6Q72L-pcDNA	Ampicillin
Rab3a-3HA-WT	Ampicillin
Rab3a-3HA-NI	Ampicillin
Rab3b-3HA-WT	Ampicillin
Rab3b-3HA-NI	Ampicillin
Rab3c-3HA-WT	Ampicillin
Rab3c-3HA-NI	Ampicillin
Rab3d-3HA-WT	Ampicillin
Rab3d-3HA-NI	Ampicillin
GFP-Rab2WT	Kanamycin
GFP-Rab2N119I	Kanamycin
Rab2a	Kanamycin
Rab3a	Kanamycin
Rab8a	Kanamycin
Rab9a	Kanamycin
Rab10	Kanamycin
Rab11a	Kanamycin
Rab6c	Kanamycin
Rab7b	Kanamycin
Rab8b	Kanamycin
Rab9b	Kanamycin

Appendix 1. Table of antibiotic resistance associated with DNA plasmid containing each Rab protein insert. Note: Rab1b sample was amplified and purified by Jody Janovick and is not included.

Rab Protein DNA Sample	260 µm Raw	280 µm Raw	320 µm Raw	260 µm	280 µm	260 µm /280 µm	ng/µL
Rab8WT-FLAG	2.662	1.547	0.325	2.311	1.204	1.92	2.311243
Rab11aN124I-flag	2.468	1.397	0.254	2.198	1.131	1.944	2.198352
Rab6Q72L-pcDNA	2.5	1.414	0.252	2.229	1.15	1.938	2.228986
Rab3a-3HA-WT	2.173	1.205	0.192	1.977	1.011	1.956	1.977209
Rab3a-3HA-NI	2.194	1.286	0.302	1.866	0.965	1.933	1.865679
Rab3b-3HA-WT	2.467	1.371	0.209	2.261	1.161	1.948	2.26123

Rab3b-3HA-NI	2.067	1.172	0.226	1.832	0.94	1.95	1.831987
Rab3c-3HA-WT	2.189	1.231	0.212	1.986	1.023	1.941	1.986278
Rab3c-3HA-NI	2.475	1.381	0.216	2.254	1.161	1.942	2.254178
Rab3d-3HA-WT	2.313	1.308	0.24	2.064	1.061	1.947	2.064461
Rab3d-3HA-NI	2.241	1.294	0.281	1.927	0.992	1.944	1.927444
GFP-Rab2WT	0.457	0.348	0.227	0.208	0.106	1.953	0.207795
GFP-Rab2N119I	0.405	0.312	0.21	0.177	0.091	1.934	0.176967
Rab2a	0.578	0.455	0.316	0.234	0.119	1.958	0.233628
Rab3a	0.53	0.437	0.324	0.171	0.089	1.933	0.17146
Rab8a	0.604	0.438	0.253	0.326	0.168	1.943	0.326467
Rab9a	0.444	0.351	0.249	0.161	0.081	2	0.161258
Rab10	0.515	0.415	0.298	0.181	0.092	1.964	0.180673
Rab11a	0.433	0.323	0.202	0.212	0.107	1.981	0.211858
Rab6c	0.426	0.324	0.211	0.197	0.102	1.933	0.197101
Rab7b	0.45	0.349	0.238	0.18	0.091	1.982	0.180125
Rab8b	0.477	0.386	0.28	0.163	0.082	1.995	0.163102
Rab9b	0.384	0.291	0.19	0.175	0.09	1.944	0.175071

Appendix 2. Absorbance data and DNA concentration values (ng/µL). Note: Rab1b sample was amplified and purified by Jody Janovick and is not included.

Rab Protein DNA Sample	Expected Size (bp)	Accession Number
Rab8WT-FLAG	624	AF498943
Rab11aN124I-flag	650	AK311770
Rab6Q72L-pcDNA	626	M28212
Rab3a-3HA-WT	662	NM002866
Rab3a-3HA-NI	662	NM002866
Rab3b-3HA-WT	659	NM002867
Rab3b-3HA-NI	659	NM002867
Rab3c-3HA-WT	683	AY026936
Rab3c-3HA-NI	683	AY026936
Rab3d-3HA-WT	659	NM004283
Rab3d-3HA-NI	659	NM004283
GFP-Rab2WT	638	M28213
GFP-Rab2N119I	638	M28213
Rab2a	639	AF498930

Rab3a	662	NM002866
Rab8a	623	NM005370
Rab9a	605	NM004251
Rab10	603	AF297660
Rab11a	650	AK311770
Rab6c	765	AB232598
Rab7b	599	NM001164522
Rab8b	612	NM016530
Rab9b	606	NM016370

Appendix 3. Table of anticipated Rab protein DNA lengths in base pairs from published literature.

Transfection Amounts

Sample	H2O (µl)	10ng hWT GnRHR (µl)	90ng Vector (µl)	90ng Rab (µl)	OPTI-MEM (µl)	Stock DNA ng/µl	Total H2O
hwt GnRHR	1.66	0.87	0.85	0.00	23.62	51.828	1.72
Rab8WT-FLAG	1.53	0.87	0.00	0.98	23.62	412.616	1.85
Rab6WT	1.53	0.87	0.00	0.98	23.62	414.32	1.85
Rab11aN124I-flag	1.70	0.87	0.00	0.81	23.62	498.593	1.68
Rab6Q72L-pcDNA	1.69	0.87	0.00	0.82	23.62	493.751	1.69
Rab3a-3HA-WT	1.60	0.87	0.00	0.91	23.62	444.579	1.78
Rab3a-3HA-NI	1.51	0.87	0.00	1.01	23.62	402.469	1.87
Rab3b-3HA-WT	1.53	0.87	0.00	0.99	23.62	411.046	1.85
Rab3b-3HA-NI	1.58	0.87	0.00	0.93	23.62	433.32	1.80
Rab3c-3HA-WT	1.55	0.87	0.00	0.97	23.62	419.569	1.83
Rab3c-3HA-NI	1.49	0.87	0.00	1.02	23.62	397.187	1.89
Rab3d-3HA-WT	1.54	0.87	0.00	0.97	23.62	416.05	1.84
Rab3d-3HA-NI	1.53	0.87	0.00	0.98	23.62	412.061	1.85
Rab1b	1.43	0.87	0.00	1.08	23.62	375.173	1.95
hwt GnRHR	1.66	0.87	0.85	0.00	23.62	51.828	1.72
vector (100ng)	2.43	0.00	0.95	0.00	23.62	475.161	0.95
GFP-Rab2WT	0.56	0.87	0.00	1.95	23.62	207.795	2.82
GFP-Rab2N119I	0.22	0.87	0.00	2.29	23.62	176.967	3.16
Rab2a	0.78	0.87	0.00	1.73	23.62	233.628	2.60
Rab3a	0.15	0.87	0.00	2.36	23.62	171.46	3.23
Rab8a	1.27	0.87	0.00	1.24	23.62	326.467	2.11
Rab9a	0.00	0.87	0.00	2.51	23.62	161.258	3.38
Rab10	0.27	0.87	0.00	2.24	23.62	180.673	3.11
Rab11a	0.60	0.87	0.00	1.91	23.62	211.858	2.78
Rab6c	0.46	0.87	0.00	2.05	23.62	197.101	2.92
Rab7b	0.26	0.87	0.00	2.25	23.62	180.125	3.12
Rab8b	0.03	0.87	0.00	2.48	23.62	163.102	3.35
Rab9b	0.20	0.87	0.00	2.31	23.62	175.071	3.18

Appendix 4: Table of prescribed amounts of components for transfection of each Rab protein DNA. Note that all samples listed below vector were only subjected to the second and third trials. DNA concentration of each sample determined the amount of Rab protein DNA added in transfections with water added to equate amounts of total solution added. The hWT GnRHR samples only received vector DNA and hWT GnRHR and vector samples only received vector DNA.

Sample	Trial 1 (Average cpm)	Trial 2 (Average cpm)	Trial 3 (Average cpm)	Average cpm	Standard error	% of hWT	% Diff.	Y-error Adjusted
Average hWT	304.605	305.17165	420.18375	343.3201333	66.72942243	100.0%	0.0%	19.437%
Rab8WT-FLAG	108.3	94.75	104.9	102.65	7.823096148	29.9%	-70.1%	7.621%
Rab6WT	381.55	349.3	483.5	404.7833333	77.48040613	117.9%	17.9%	19.141%
Rab11aN124I-flag	289.6	143.8667	283.8	239.0889	84.13915998	69.6%	-30.4%	35.192%
Rab6Q72L-pcDNA	268.05	251.35	287.85	269.0833333	21.07328483	78.4%	-21.6%	7.832%
Rab3a-3HA-WT	522.51	349.8025	615.21	495.8408333	153.2330916	144.4%	44.4%	30.904%
Rab3a-3HA-NI	457.81	397.31	591.91	482.3433333	112.3523624	140.5%	40.5%	23.293%
Rab3b-3HA-WT	329.7575	267.655	391.26	329.5575	71.36338002	96.0%	-4.0%	21.654%
Rab3b-3HA-NI	282.7575	X	388.61	335.68375	61.11396937	97.8%	-2.2%	18.206%
Rab3c-3HA-WT	275.9575	277.81*	352.41	314.18375	44.13987146	91.5%	-8.5%	14.049%
Rab3c-3HA-NI	397.56	X	332.81	365.185	37.38342993	106.4%	6.4%	10.237%
Rab3d-3HA-WT	266.1075	228*	231.21	248.65875	20.14808102	72.4%	-27.6%	8.103%
Rab3d-3HA-NI	330.21	285.81	361.01	325.6766667	43.41674024	94.9%	-5.1%	13.331%
Rab1b	178.91	195.4025	173.3575	182.5566667	12.72768668	53.2%	-46.8%	6.972%
vector	71.1	80.9	88.8	80.26666667	10.21909976	23.4%	-76.6%	12.731%
GFP-Rab2WT	X	109.25	126.5075	117.87875	9.963622271	34.3%	-65.7%	8.452%
GFP-Rab2N119I	X	139.1525	131.2575	135.205	4.558180375	39.4%	-60.6%	3.371%
Rab2a	X	122.8525	146.8075	134.83	13.8304257	39.3%	-60.7%	10.258%
Rab3a	X	169.81	170.11	169.96	0.173205081	49.5%	-50.5%	0.102%
Rab8a	X	108.65	110.36	109.505	0.98726896	31.9%	-68.1%	0.902%
Rab9a	X	175.91	168.11	172.01	4.5033321	50.1%	-49.9%	2.618%
Rab10	X	141.66	175.36	158.51	19.45670407	46.2%	-53.8%	12.275%
Rab11a	X	142.96	163.21	153.085	11.69134295	44.6%	-55.4%	7.637%
Rab6c	X	162.06	171.51	166.785	5.455960044	48.6%	-51.4%	3.271%
Rab7b	X	121.76	130.46	126.11	5.022947342	36.7%	-63.3%	3.983%
Rab8b	X	118.21	105.36	111.785	7.418950959	32.6%	-67.4%	6.637%
Rab9b	X	129.56	122.41	125.985	4.128054425	36.7%	-63.3%	3.277%
hWT GnRHR	316.8	272.3333	391.8	326.9777667	68.9741314	95.2%	-4.8%	21.094%
hWT GnRHR	292.41	338.01	448.5675	359.6625	90.15757466	104.8%	4.8%	25.067%

Appendix 4. Raw data showing average radioactivity (cpm) in each Rab protein transfection sample. Twelve protein samples were added for Trials 2 and 3. Values were averaged and then divided by the average production of control, hWT GnRHR samples with no added Rab protein. Percent difference was calculated and y-error bars adjusted to show range of potential error. *All but one well of these samples were compromised during Trial 2. X denotes that a trial was not performed, or samples were thrown out due to known experimental error. In the case of Rab3b-3HA-NI and Rab3c-3HA-NI all wells were compromised.